# X-raying the winds of the evolved massive binary HDE228766

G. Rauw, L. Mahy, Y. Nazé
University of Liège, Belgium

## Introduction :

HDE228766 is an evolved massive binary hosting a rare Of-WN8ha transition star on a circular orbit about an O7 star (Rauw et al. 2002). To probe the wind of the transition star, we have obtained XMM-Newton EPIC spectra at three key orbital phases .

## XMM-Newton observations of HDE228766:

We have obtained observations at phases 0.00, 0.50 and 0.75 (see Fig. 1). At **φ = 0.0, our line of sight to the wind-interaction zone crosses the wind of the transition star**. At φ = 0.5, the O7 star is in front and our line of sight crosses the less dense and less chemically enriched wind of the O7 star.

The EPIC spectra show clear differences between the three phases, the spectrum at φ = 0.0 showing the lowest level of X-ray emission and the one at φ = 0.5 displaying the highest level of emission (see Fig. 2 and 3).

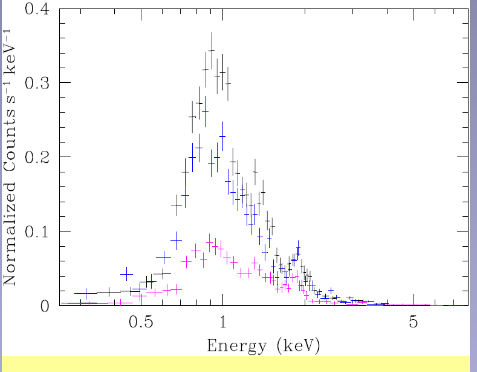


Fig.2: EPIC-pn spectra of HDE228766 at φ = 0.0 (magenta), φ = 0.50 (black) and φ = 0.75 (blue).

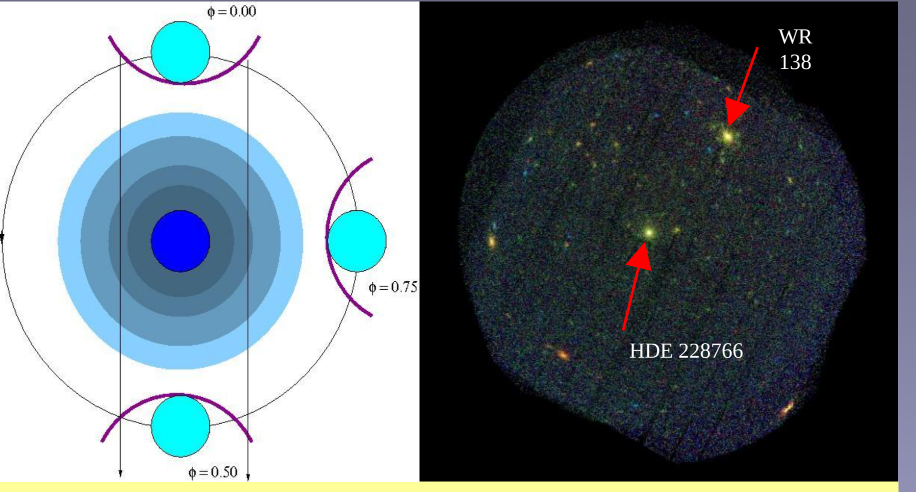


Fig.1, left: schematic illustration of the orbital configuration of the O7 star at the times of the X-ray observations. The observer is at the bottom. Right: combined EPIC image of the FoV around HDE228766. The X-ray spectra of WR138 were analyzed by Palate et al. (2013).

The EPIC spectra were adjusted with 2-T thermal plasma models (Rauw et al. 2014) confirming that **the variations are due to changing wind optical depth**. The results of the fits are listed in the Table below and the ratio between the observed fluxes at different orbital phases is shown in Fig. 3.

| Obs | $\phi$ | Model | $\log N_{wind,1}$ ($cm^{-2}$) | $\tau_{wind,1}$ | $10^4\times$ norm$_1$ ($cm^{-5}$) | $\log N_{wind,2}$ ($cm^{-2}$) | $\tau_{wind,2}$ | $10^4\times$ norm$_2$ ($cm^{-5}$) | $\chi^2_\nu(\nu)$ | $f_X$ ($10^{-13}$ erg cm$^{-2}$ s$^{-1}$) | $f_X^{un}$ ($10^{-13}$ erg cm$^{-2}$ s$^{-1}$) |
|---|---|---|---|---|---|---|---|---|---|---|---|
| I | 0.75 | 2 | $21.65^{+.68}$ | 0.11 | $4.2^{+3.5}_{-.9}$ | $22.74^{+.06}_{-.05}$ | 1.38 | $7.19^{+.49}_{-.56}$ | 1.75(115) | $3.67^{+.01}_{-.54}$ | 13.4 |
| II | 0.50 | 1 | $21.88^{+.17}_{-.48}$ | 0.50 | $9.2^{+4.4}_{-3.9}$ | $22.16^{+.06}_{-.06}$ | 0.96 | $6.88^{+.60}_{-.62}$ | 1.40(119) | $4.55^{+.03}_{-.18}$ | 17.5 |
| III | 0.00 | 2 | $22.53^{+.23}$ | 0.85 | $3.9^{+4.6}_{-2.8}$ | $22.92^{+.11}_{-.09}$ | 2.09 | $4.00^{+.53}_{-.55}$ | 1.29(91) | $1.58^{+.02}_{-.14}$ | 4.7 |

## A toy model of the wind collision zone

Using the formalism of Cantó et al. (1996), we have computed the shape of the wind interaction zone (Fig. 4) and modeled its X-ray emission absorbed by the overlaying wind material. Wind opacities were computed with the CMFGEN model atmosphere code (Hillier & Miller 1998) and then integrated along the line of sight for a grid of values of the wind parameters ($\dot{M}$ and $v_\infty$) of both stars and the orbital inclination (i) and for different assumptions on the maximum radius of the X-ray emission zone (see Fig. 4).

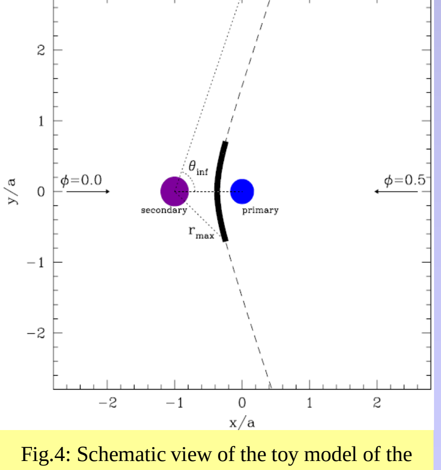


Fig.4: Schematic view of the toy model of the wind interaction region. The primary star is the O7 component, whilst the secondary star is the Of-WN8ha transition star. The X-ray emission zone is shown by the thick part of the wind interaction region.

Models that reproduce the observed flux ratios and wind optical depths at 1 keV **have i = 54 – 61°**, implying a mass of 47 – 60 $M_{Sun}$ for the transition star. They also indicate that the **wind momentum ($\dot{M} \times v_\infty$) of the transition star is at least 5 times larger than that of the O7 companion.** Finally, we find that the maximum radius of the X-ray emission zone $r_{max}$ **lies between 0.5 and 1.5 times the orbital separation.**

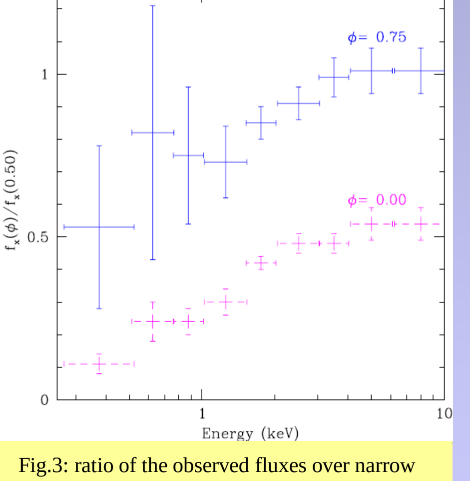


Fig.3: ratio of the observed fluxes over narrow energy bands with respect to those at phase 0.50.

## References:

Cantó, J., Raga, A.C., & Wilkin, F.P. 1996, ApJ 469, 729
Hillier, D.J., & Miller D.L. 1998, ApJ 496, 407
Palate, M., Rauw, G., De Becker, M., Nazé, Y., & Eenens, P. 2013, A&A 560, A27
Rauw, G., Crowther, P.A., Eenens, P., Manfroid, J., & Vreux, J.-M. 2002, A&A 392, 563
Rauw, G., Mahy, L., Nazé, Y., Eenens, P., Manfroid, J., & Flores, C.A. 2014, A&A 566, A107